2012

Improved particle statistics for laser-plasma self-injection simulations

B W. Cowan
Tech-X Corporation

Serguei Y. Kalmykov
University of Nebraska-Lincoln, s.kalmykov.2013@ieee.org

Bradley Allan Shadwick
University of Nebraska-Lincoln, shadwick@unl.edu

K Bunkers
University of Nebraska-Lincoln

D L. Bruhwiler
Tech-X Corporation

See next page for additional authors

Improved particle statistics for laser-plasma self-injection simulations

B. M. Cowan[*], S. Y. Kalmykov[†], B. A. Shadwick[†], K. Bunkers[†], D. L. Bruhwiler[*,**] and D. P. Umstadter[†]

[*]*Tech-X Corporation, 5621 Arapahoe Ave., Boulder, CO 80303*
[†]*Department of Physics and Astronomy, University of Nebraska – Lincoln, NE 68588-0299*
[**]*Present address: 1348 Redwood Ave., Boulder, CO 80304*

Abstract. We describe methods for improving the accuracy of injected particle beams by selectively enhancing the particle statistics in particle-in-cell simulations, using reduced model computations as a guide. We demonstrate convergence of key beam parameters in two dimensions, and show improved noise properties in three dimensions.

INTRODUCTION

Laser-plasma accelerators (LPAs) are capable of producing both accelerating gradients and transverse focusing forces several orders of magnitude higher than conventional accelerators [1, 2]. The field of LPA has made significant strides in the last decade, including the demonstration of high-quality ∼100 MeV electron bunches from a laser-plasma interaction [3–5] and several years later the production of GeV-scale beams [6–9]. With these advances have come interest in a broad range of applications. In particular, realization of compact, inexpensive, bright x- and gamma-ray sources using electron beams from LPAs [10–12] holds the promise to enable a much wider user community than can be served by existing large-scale facilities. Some of these applications have very tight beam requirements, including generating coherent x-rays using an external magnetic undulator [13–15], producing x-rays for phase contrast imaging [16, 17], and high-brightness, quasi-monochromatic gamma-ray Compton sources [18, 19]; these require electron beams with a multi-kA current, low phase space volume, and energy in the few-GeV range.

There are several mechanisms by which LPA interactions can generate quasi-monoenergetic electron bunches. One of these, and the one we focus on here, is self-injection in the so-called blowout (or "bubble") regime [20]. In this case, the laser pulse is intense enough that it completely expels all the plasma electrons from its vicinity, and the wake fields are sufficiently strong to produce injection. Other methods, such as colliding pulses [21] and plasma density gradients [22], have been investigated to provide further control over the injection process. For the purposes of x-ray generation, the bubble regime has several advantages. First, it does not require additional laser pulses, precise density profiles, or a separately produced channel. Second, self-injection in the bubble regime can produce, in a single stage, bunches in the energy range most relevant for x-ray generation, namely ∼100 MeV to several GeV. Third, simulations have shown that stable beam parameters can be achieved for multi-GeV bunches [23, 24]. Finally, the ion channel free of electrons created in the bubble regime provides linear focusing for the injected electrons, allowing minimal emittance growth during acceleration.

Throughout the history of laser-plasma acceleration, simulations have played a role in the planning of LPA experiments and interpretation of the results. In particular, large-scale two-dimensional (2D) and three-dimensional (3D) electromagnetic particle-in-cell (PIC) simulations [25, 26] have been indispensable for recent developments, providing essential understanding of the dynamical processes involved [9, 24, 27–30]. As applications demand ever greater control over the injected bunch parameters, a greater degree of quantitative accuracy is needed in simulations to inform LPA system designs. One common source of numerical error in PIC simulations is the lack of sufficient particle statistics; that is, the simulation does not include enough macroparticles to accurately represent the physical particle phase space. Since PIC simulations of LPA are inherently computationally expensive, the challenge is to improve particle statistics without significantly increasing the computational burden.

In this report we present two methods for improving particle statistics in LPA simulations. The first approach treats the beam using conventional PIC particles, taking advantage of our knowledge of their initial coordinates to load a greater number of macroparticles in that region. The other method is a novel approach in which particles track their

Advanced Accelerator Concepts
AIP Conf. Proc. 1507, 375-380 (2012); doi: 10.1063/1.4773725

own deformations and split as they expand so as to automatically generate greater statistics. In the following sections, we describe these methods and demonstrate their effectiveness in the PIC code VORPAL [31].

ENHANCED LOADING

Our first method consists of enhancing the loading of macroparticles in the region, dubbed the *collection volume*, where the injected particles originate. Tracking initial positions of the beam particles [24, 28–30, 32] shows that the collection volume is a thin cylindrical shell, symmetric with respect to the propagation axis, having a radius approximately the same as the spot size of the driving laser pulse. A reduced model simulation can be used initially to determine the collection volume with sufficient accuracy for this technique [32]. In our method, we check whether the center of a cell is within the collection volume, and if so, load a higher number of macroparticles in that cell.

We find that enhanced loading provides quantitative convergence of key particle beam parameters and reveals important features of the beam, while still saving computation time compared to the usual method of uniform loading. The bulk of our testing was with two-dimensional simulations, so we first note that unlike in 3D simulations, in our 2D model we observed injection primarily in the second bucket. In addition, a completely evacuated bubble is not formed in the second bucket, so we do not obtain linear focusing. Both of these effects can be seen with enhanced loading, and only in full detail with higher particle statistics.

To test enhanced loading, we first conducted a benchmark simulation using physical parameters known to show injection. For this benchmark, we used typical numerical parameters for simulations without improved particle statistics, including particle loading of 1 particle per cell (PPC) longitudinally and 3 transversely throughout the simulation volume. We then extracted the collection volume and used this as our region of enhanced loading in our subsequent tests.

We conducted simulations with just 1 PPC outside the collection volume, but 1, 2, 4, 8, and 16 PPC inside the collection volume, equally spaced transversely. After 1.28 mm of propagation, the longitudinal phase space of the self-injected beam has rotated to the point of minimal energy spread. We plot this longitudinal phase space for our benchmark simulation and the enhanced loading simulations in Fig. 1. We immediately observe one very distinct feature of these beams: The benchmark simulation and the test simulations with poor statistics show injection in the first bucket as well. However, as enhanced loading improves the particle statistics, this first-bucket beam eventually disappears. Injection into the first bucket is thus entirely due to numerical noise, and significantly enhanced loading in the collection volume—more that 4 PPC—is required to eliminate it.

From our simulations we extracted figures of merit of the bunch injected in the second bucket for our convergence study. These included bunch charge, mean longitudinal momentum, longitudinal momentum spread, and transverse emittance, which are plotted in Fig. 2. We find excellent convergence in charge and mean momentum, with the relative difference of the two highest statistics cases less than 0.4% for both quantities; for momentum the relative difference among the 4, 8, and 16 PPC tests is less than 1%. The convergence is also reasonably good for momentum spread and transverse emittance, with a relative difference in both quantities of $< 3\%$ between the highest statistics cases. Note that we do not expect a smooth convergence trend to extend to the lower statistics cases, since the injected charge in the first bucket in these cases can qualitatively affect the dynamics in the second bucket via beam loading.

We also observe the transverse phase space of the second bucket beams, plotted in Fig. 3. In these plots we can see the effect of nonlinear focusing in the spiral patterns in the halo of the particle phase space. This significant feature of the transverse distributions is slightly visible in the benchmark case, and is not clearly visible with enhanced loading until the particle statistics are increased to 8 or 16 PPC. It is worth noting that the convergence in emittance shown above is surprisingly good, given the non-Gaussian nature of the phase space distribution.

In addition, we conducted a 3D test of enhanced loading to compare to a run with uniform loading. The uniform simulation used 4 PPC everywhere, spaced evenly with 2 PPC in each transverse direction; the details of this simulation are documented in [32]. For the enhanced loading run, we loaded 16 PPC ($1\times4\times4$, evenly spaced) inside the collection volume and 1 PPC outside. In this simulation, a bunch was injected into the first plasma bucket, and injection was terminated by bubble contraction after 1.24 mm of laser propagation; we observe the injected bunch at that point. We find generally better statistics in the injected beam with enhanced loading. As an example, we plot the transverse phase space in the y direction for both simulations in Fig. 4. We can clearly see improved statistics in the enhanced loading data, resulting in a smoother distribution. We also see better representation of the beam halo; the visible patterns could help diagnose nonlinear effects in design studies.

A remarkable aspect of the enhanced loading procedure is that these clear benefits come with substantial savings in computational resources. In fact, the enhanced loading 3D simulation loaded 68% fewer total particles than the

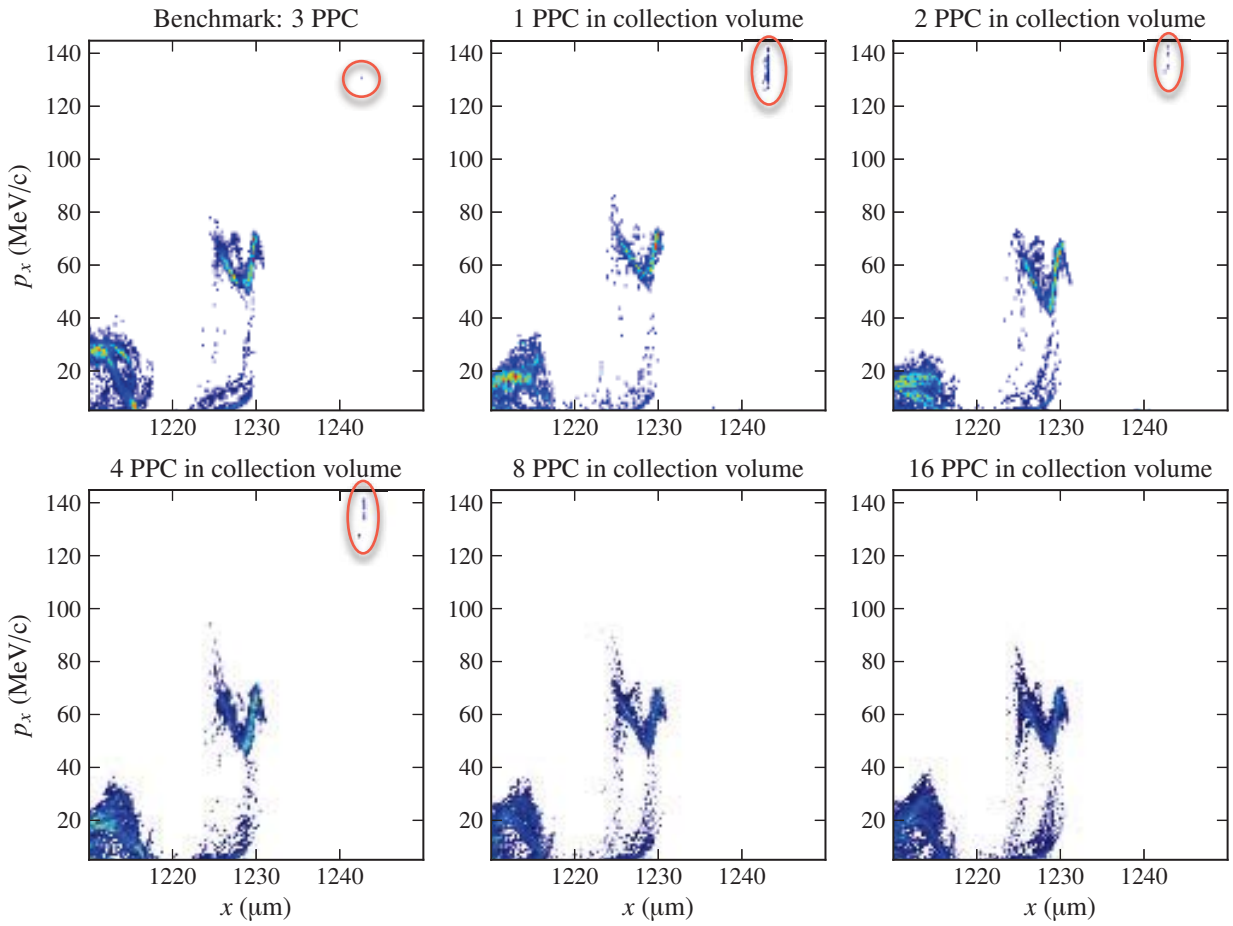

FIGURE 1. (Color online) Longitudinal phase space of accelerated particles at the point of minimal energy spread. These plots contain all particles with $\beta_x\gamma \geq 10$, many of which are not part of the beam. The beam in the second bucket is visible as the particles with longitudinal momentum over 40 MeV/c. Particles injected in the first bucket in low-statistics simulations are indicated in the red ovals.

uniform loading simulation, while delivering superior beam statistics. The enhanced loading simulation indeed ran slightly faster than the uniform loading run even with no attempt at optimization or parallel load balancing.

Thus, through enhanced loading of macroparticles in the collection volume of an LPA self-injection simulation, we have shown both improved description of the qualitative features of an accelerated bunch and good quantitative convergence. As an added benefit, these improvements come with computational speedup.

BLOB PARTICLES

As an alternative to the enhanced loading, we implemented in VORPAL the "blob" particle method, which tracks deformations of particle phase space. This allows PIC macroparticles to change shape as they propagate, and to split when their spatial extent becomes too large. Our method is based on previous work on methods in which macroparticles represent distributions in phase space [33–35]. Those methods have generally been aimed at systems in which the velocity distributions are primarily Maxwellian. In our case, we have an initially cold plasma, and the energies acquired by the particles due to the laser pulse are much greater than any thermal energy that develops. We therefore adapt these methods so that individual macroparticles do not contain any thermal velocity spread. Since the benefits of this algorithm are less clear than those for enhanced loading, we just summarize the method and results here.

In our algorithm, the macroparticle deformations are stored and updated via additional dynamic variables consisting

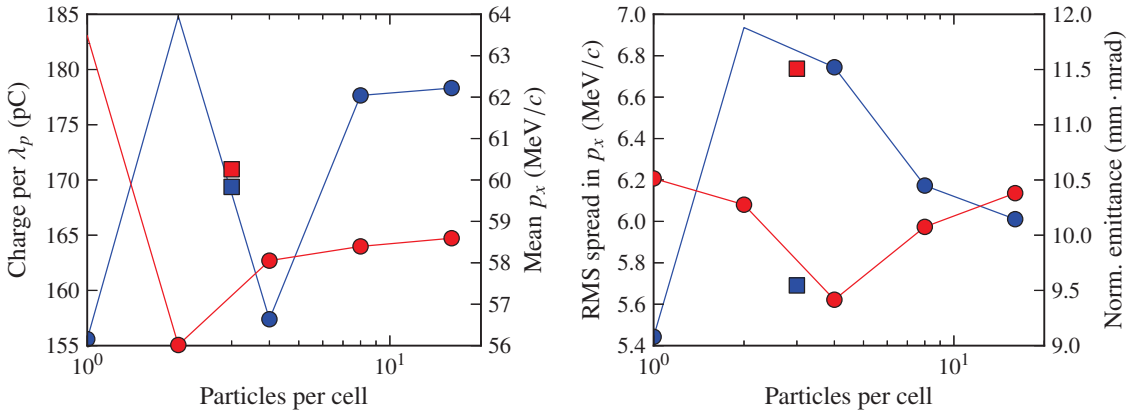

FIGURE 2. (Color online) Left: Bunch charge [blue (light gray)] and mean longitudinal momentum [red (gray)] of the second-bucket bunch. Note that in these two-dimensional simulations, the integrated charge value represents the charge per unit length in the third dimension. We therefore normalize the charge to the amount in one plasma wavelength, to obtain values comparable to the 3D case, and plot those values here. Right: Longitudinal momentum spread [blue (light gray)] and normalized transverse emittance [red (gray)]. In both the left and right plots, the circles represent enhanced loading runs with the given number of particles per cell inside the collection volume and 1 PPC elsewhere, while the squares represent the benchmark case of 3 PPC everywhere.

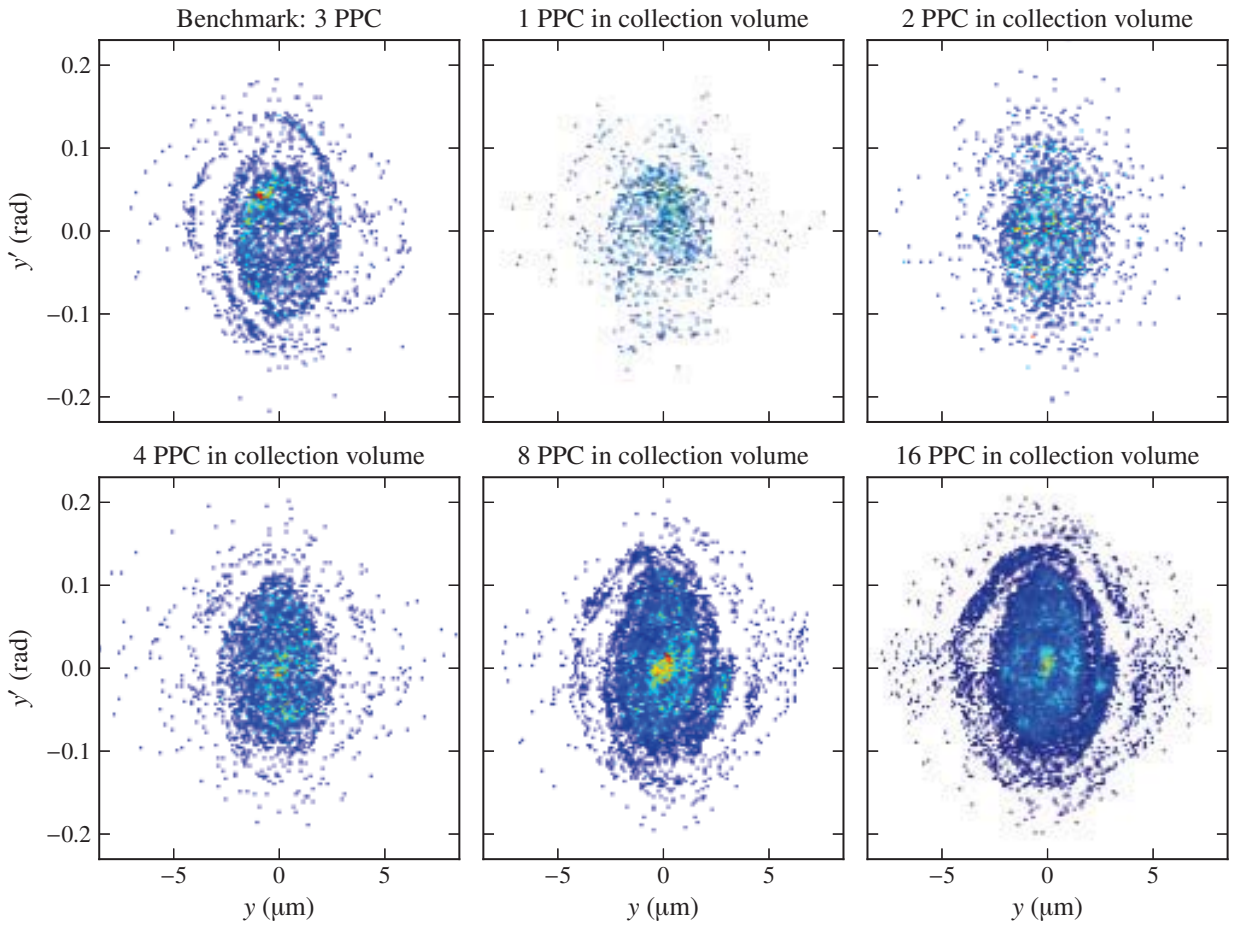

FIGURE 3. (Color online) Transverse phase space of particles injected into the second bucket and accelerated after 1.28 mm.

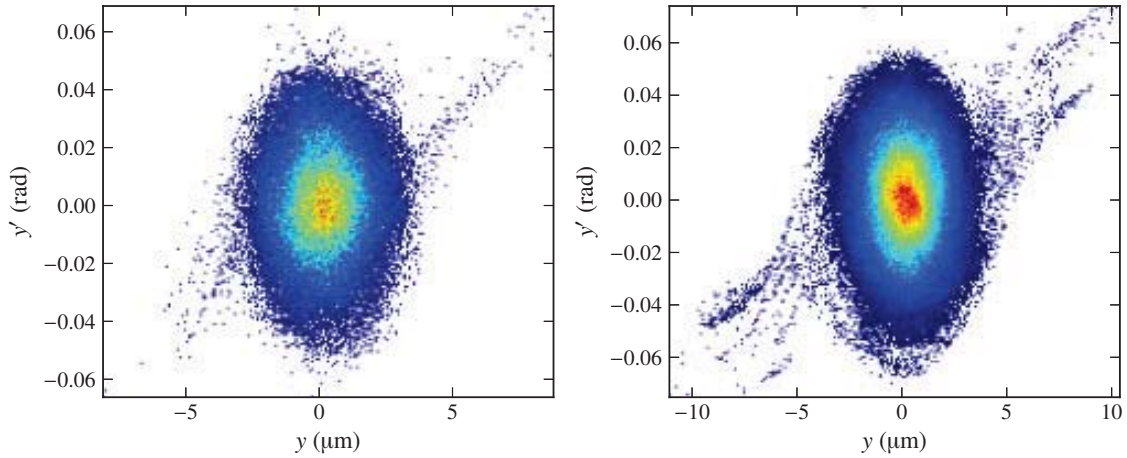

FIGURE 4. (Color online) Transverse y-y' phase space of a particle bunch in a 3D self-injection simulation. Left: uniform loading; right: enhanced loading.

of the matrix elements of two linear maps. These maps track deformations of position and velocity in terms of an original displacement from the center of the macroparticle. These maps are updated in a straightforward way using the spatial derivatives of the electromagnetic fields. The trickier part of the blob particle algorithm is the current deposition procedure, made difficult by the fact that once a particle is deformed, its shape function is no longer separable along the coordinate axes. We overcame this challenge by changing the integration region for charge deposition in each cell to a parallelepiped with the same axes as the deformed particle and bounding the desired cell.

The final aspect of the blob particle algorithm is the particle splitting procedure. The growth of a macroparticle's spatial extent reflects that the physical plasma particles the macroparticle represents cover a larger region of space. As the growth increases, the representation of those physical particles by a single macroparticle becomes poorer. Therefore, once a macroparticle grows by a certain amount in any direction, we split it into several macroparticles to better represent the physical particle phase space.

We obtained some remarkable results in our tests of the blob particle algorithm. We used the same two-dimensional parameters as in the tests of enhanced loading described above. We conducted a single test simulation, beginning with 1 PPC, the idea being that particle splitting will generate particle statistics exactly where the dynamics demand it, providing an accurate representation of the particle beam. While the quantitive benefits of this method are not yet as clear as those for enhanced loading, the qualitative results indicate some distinct advantages.

In comparing the figures of merit with the enhanced loading results shown in Fig. 2, we see some large differences. We find ~30% higher mean longitudinal momentum but with ~50% less momentum spread, much lower charge—by a factor of 6—and slightly higher transverse emittance. In addition, we observed in the longitudinal phase space that the blob algorithm does not eliminate injection into the first bucket. In some basic testing we did observe some noise due to the splitting process, and it is possible that such noise is responsible for the first-bucket injection. However, despite the noise, we also observed that the blob particles ultimately occupy a much smaller region of phase space than conventional particles. This is apparent from the lower energy spread, as well as the transverse phase space. Compared to the conventional particles, we found that the structure of the transverse phase space due to nonlinear effects is much more apparent. Therefore the blob method may provide some insight into the details of of the LPA injection process not available from conventional PIC. Thus, we conclude that while not proven, the blob method exhibits some interesting properties.

CONCLUSION

We have shown significant benefits, in both qualitative and quantitative accuracy, from enhanced loading, including convergence of key bunch parameters, while at the same time conserving computational resources. We have also seen some advantageous features in the results of blob particle tests.

ACKNOWLEDGMENTS

The authors wish to thank D. N. Smithe for helpful advice. The work of B. M. C. and D. L. B. was supported by U. S. DOE Contract DE-SC0006245 (SBIR). The work of S. Y. K. and B. A. S. was in part supported by U. S. DOE Grants DE-FG02-08ER55000 and DE-SC0008382 and NSF grant PHY-1104683. The work of S. Y. K., B. A. S., and D. P. U. was also in part supported by U. S. DOE Grant DE-FG02-05ER15663, DTRA Contract HDTRA1-11-C-0001, and AFOSR Grants FA9550-11-1-0157 and 9550-08-1-0232. VORPAL simulations used resources of the National Energy Research Scientific Computing Center, which is supported by the Office of Science of the U. S. DOE under Contract No. DE-AC02-05CH11231.

REFERENCES

1. T. Tajima and J. M. Dawson, *Phys. Rev. Lett.* **43**, 267–270 (1979).
2. E. Esarey, C. B. Schroeder, and W. P. Leemans, *Rev. Mod. Phys.* **81**, 1229–1285 (2009).
3. C. G. R. Geddes et al., *Nature* **431**, 538–541 (2004).
4. S. P. D. Mangles et al., *Nature* **431**, 535–538 (2004).
5. J. Faure et al., *Nature* **431**, 541–544 (2004).
6. W. P. Leemans et al., *Nature Phys.* **2**, 696–699 (2006).
7. S. Kneip et al., *Phys. Rev. Lett.* **103**, 035002 (2009).
8. D. H. Froula et al., *Phys. Rev. Lett.* **103**, 215006 (2009).
9. S. Banerjee et al., *Physics of Plasmas* **19**, 056703 (2012).
10. A. Rousse et al., *Phys. Rev. Lett.* **93**, 135005 (2004).
11. A. Rousse et al., *Eur. Phys. J. D* **45**, 391–398 (2007).
12. S. Kneip et al., *Nature Phys.* **6**, 980–983 (2010).
13. F. Grüner et al., *Appl. Phys. B* **86**, 431–435 (2007).
14. H.-P. Schlenvoigt et al., *Nature Phys.* **4**, 130–133 (2008).
15. M. Fuchs et al., *Nature Phys.* **5**, 826–829 (2009).
16. S. Fourmaux et al., *Opt. Lett.* **36**, 2426–2428 (2011).
17. S. Kneip et al., *Appl. Phys. Lett.* **99**, 093701 (2011).
18. W. Leemans et al., *IEEE Trans. Plasma Sci.* **33**, 8–22 (2005).
19. F. V. Hartemann et al., *Phys. Rev. ST Accel. Beams* **10**, 011301 (2007).
20. W. Lu et al., *Phys. Rev. ST Accel. Beams* **10**, 061301 (2007).
21. J. Faure et al., *Nature* **444**, 737–739 (2006).
22. C. G. R. Geddes et al., *Phys. Rev. Lett.* **100**, 215004 (2008).
23. S. F. Martins et al., *Nature Phys.* **6**, 311 (2010).
24. S. Y. Kalmykov et al., *New J. Phys.* **12**, 045019 (2010).
25. R. W. Hockney and J. W. Eastwood, *Computer Simulation Using Particles*, McGraw-Hill, New York, NY, 1981.
26. C. K. Birdsall and A. B. Langdon, *Plasma Physics via Computer Simulation*, McGraw-Hill, New York, NY, 1985.
27. H. Xu et al., *Phys. Plasmas* **12**, 013105 (2005).
28. H.-C. Wu et al., *Phys. Plasmas* **16**, 073108 (2009).
29. S. Y. Kalmykov et al., *Phys. Plasmas* **18**, 056704 (2011).
30. S. Y. Kalmykov et al., *New J. Phys.* **14**, 033025 (2012).
31. C. Nieter and J. R. Cary, *J. Comput. Phys.* **196**, 538 (2004).
32. B. M. Cowan et al., *J. Plasma Phys.* (2012), "Computationally efficient methods for modelling laser wakefield acceleration in the blowout regime," available on CJO doi:10.1017/S0022377812000517.
33. D. J. Larson, *J. Comput. Phys.* **188**, 123–138 (2003).
34. D. W. Hewett, *J. Comput. Phys.* **189**, 390–426 (2003).
35. G. G. M. Coppa et al., *J. Comput. Phys.* **127**, 268–284 (1996).